Title

Cytoplasmic ATP Inhibition of CLC-1 Is Enhanced by Low pH

Journal

The Journal of General Physiology, 130(2)

ISSN

0022-1295

Authors

Tseng, Pang-Yen
Bennetts, Brett
Chen, Tsung-Yu

Publication Date

2007-08-01

DOI

10.1085/jgp.200709817

Peer reviewed

Cytoplasmic ATP Inhibition of CLC-1 Is Enhanced by Low pH

Pang-Yen Tseng,[1] Brett Bennetts,[2] and Tsung-Yu Chen[1]

[1]Center for Neuroscience and Department of Neurology, University of California, Davis, CA 95616
[2]St. Vincent's Institute, Fitzroy, Victoria 3065, Australia

The CLC-1 Cl^- channel is abundantly expressed on the plasma membrane of muscle cells, and the membrane potential of muscle cells is largely controlled by the activity of this Cl^- channel. Previous studies showed that low intracellular pH increases the overall open probability of recombinant CLC-1 channels in various expression systems. Low intracellular pH, however, is known to inhibit the Cl^- conductance on the native muscle membrane, contradicting the findings from the recombinant CLC-1 channels in expressed systems. Here we show that in the presence of physiological concentrations of ATP, reduction of the intracellular pH indeed inhibits the expressed CLC-1, mostly by decreasing the open probability of the common gate of the channel.

The Journal of General Physiology

INTRODUCTION

The generation of action potentials in excitable cells requires that the magnitude of Na^+ current on the surface membrane be large enough to overcome the electrical shunting current through other membrane conductance. Multiple action potentials raise extracellular K^+ concentrations, leading to a depolarization of membrane potential, and consequently an inactivation of voltage-gated Na^+ channels, a mechanism thought to be underlying muscle fatigue (Sejersted and Sjogaard, 2000). Recent studies, however, showed that fatigue muscles become acidified, and this cytoplasmic acidification results in reduced Cl^- conductance, a major conductance determining the membrane potential of muscle cells (Pedersen et al., 2004; Pedersen et al., 2005). The decrease of Cl^- conductance on muscle membranes thus could reduce the shunting current on the muscle membrane, providing a mechanism to overcome muscle fatigue (Pedersen et al., 2005).

Low pH has long been known to reduce the Cl^- conductance of the surface membrane of intact skeletal muscle fibers (Hutter and Warner, 1967a,b; Palade and Barchi, 1977). CLC-1, a member of the CLC channel/transporter family (Steinmeyer et al., 1991), provides the major Cl^- conductance in muscle fiber surface membranes, as evidenced from the disease myotonia congenita caused by CLC-1 mutations (Koch et al., 1992). Previous studies of the recombinant CLC-1 channel, however, showed that low intracellular pH appeared to increase the activity of CLC-1 (Rychkov et al., 1996; Accardi and Pusch, 2000), thus contradicting the observation on the native muscle cells. CLC-1 has been shown to be inhibited by intracellular ATP through a shift of the common-gate activation curve (Bennetts et al., 2005). Here we show that the ATP inhibition of CLC-1 is enhanced by low pH. In the presence of physiological concentration of ATP, reducing intracellular pH indeed inhibits the activity of recombinant CLC-1 channels. Such an inhibition may be the underlying mechanism for the low pH–induced reduction of the Cl^- conductance in native muscle membranes (Pedersen et al., 2005).

Correspondence to Tsung-Yu Chen: tycchen@ucdavis.edu

MATERIALS AND METHODS

The human CLC-1 Cl^- channel constructed in the pTLN vector was used for mRNA synthesis using SP6 mMessage mMachine kit (Ambion). The procedures for harvesting and injecting *Xenopus* oocytes were published previously (Chen, 1998; Li et al., 2005). From 3–5 d after RNA injections, excised inside-out patch recordings were performed, using the Axopatch 200B amplifier, and the Digidata 1320 A/D board controlled by pClamp8 software (Axon Instruments, Inc./Molecular Devices). The recording electrodes had a tip diameter of 7–9 μm, and had a resistance of 0.4–0.6 MΩ when filled with a pipette (extracellular) solution containing (in mM) 120 NMG-Cl, 1 $MgCl_2$, 10 HEPES, 1 EGTA, pH 7.4. The bath (intracellular) solutions had the same ionic components, with pH being adjusted to three values (7.4, 6.8, and 6.2) after the desired concentrations of ATP were added. Mg^{2+}-ATP was purchased from Sigma-Aldrich. A stock solution of 100 mM was made in distilled water, and was stored at −20°C. Working solutions of ATP were made on the same day of the experiments.

Macroscopic CLC-1 current was elicited using two voltage protocols (protocol A and B, respectively). In protocol A, the membrane potential was stepped from the 0-mV holding voltage to various test voltages from +120 to −140 mV (in −20-mV steps) for 300 ms, followed by a tail voltage at −100 mV for 300 ms. The initial value of the tail current was determined by fitting the tail current with a double-exponential function. The initial tail current of each trace was normalized to the maximal value of the initial tail current obtained following the most positive test voltage in the absence of ATP. The normalized, initial, tail current obtained using protocol A (see Fig. 1) represents the product of the open probability (P_o) of the fast gate (P_o^f) and that of the common gate (P_o^c) at the preceding test voltage (Accardi and Pusch, 2000; Duffield et al., 2003; Bennetts et al., 2005). A second voltage protocol (protocol B) was also applied to the same patch immediately following the protocol A experiment. Protocol B is exactly the same as protocol A, except a 400-μs voltage step to +170 mV

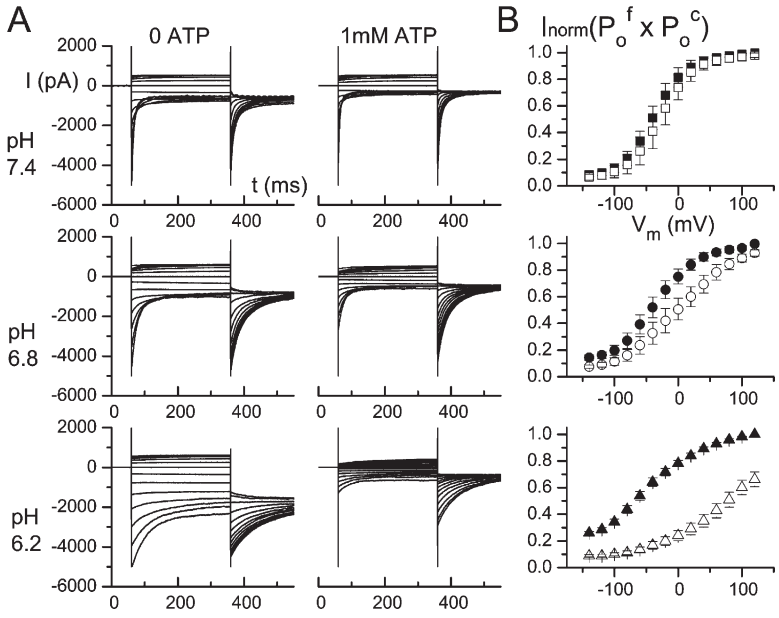

Figure 1. Effects of 1 mM cytoplasmic ATP on CLC-1 at three intracellular pH conditions. (A) Recording traces were obtained in the indicated pH and ATP conditions using voltage protocol A. (B) Normalized current (I_{norm}) represents the initial, tail current normalized to the maximal initial current in the absence of ATP. Each data point is the average from 3–6 patches. This I_{norm} value reflects the product of the fast-gate P_o and the common-gate P_o, namely $P_o^f \times P_o^c$. Solid and open symbols were in 0 and 1 mM cytoplasmic ATP, respectively.

was inserted between the test voltage and the tail voltage (Accardi and Pusch, 2000; Duffield et al., 2003; Bennetts et al., 2005). Because a short, but very positive, voltage step is enough to fully open the fast gate (but not altering the common gate, which has a slower kinetics), the normalized, initial tail current (see Fig. 2) represents P_o^c at the preceding test voltage. Dividing the value of $P_o^f \times P_o^c$ (from protocol A) by P_o^c (from protocol B) also gave an estimate of P_o^f.

To monitor the change of P_o^c upon ATP wash-in and wash-out (Fig. 4), the tail current was measured at −120 mV, following a +40-mV test voltage and the +170-mV short pulse. Solution exchange is achieved by using the SF-77 solution exchanger (Warner Instruments) as described in previous studies (Zhang et al., 2006). Data analyses and presentations were performed using the combination of pClamp8 and Origin software (Origin Lab, Co.). Data points were presented as mean ± SEM. The $V_{1/2}$ of the P_o-V curve was obtained by fitting the data points to a Boltzmann equation.

RESULTS

For every excised patch, we applied voltage protocol A and protocol B to examine the functions of CLC-1. Fig. 1 A shows recording traces in the absence and presence of 1 mM cytoplasmic ATP at three pH conditions, using voltage protocol A. The normalized value of the initial tail current, which represents the overall channel

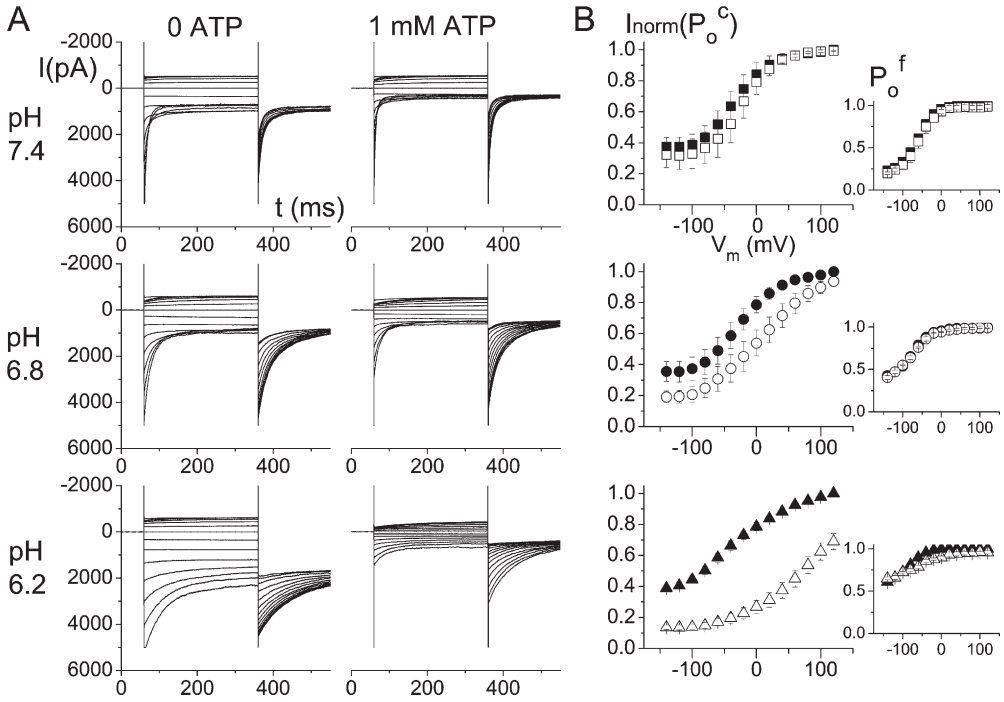

Figure 2. Effects of 1 mM ATP on the common gate of CLC-1. (A) Recording traces obtained in the indicated conditions using voltage protocol B. (B) Normalized value of the initial tail current (I_{norm}) in each pH condition (as shown in A). This I_{norm} value has been widely used to represent the P_o of the common gate (P_o^c). Dividing the I_{norm} in Fig. 1 B (from protocol A) by the I_{norm} here (from protocol B) gives the fast-gate P_o (P_o^f), which is shown in the inset of each panel. Solid and open symbols were obtained in 0 and 1 mM cytoplasmic ATP, respectively.

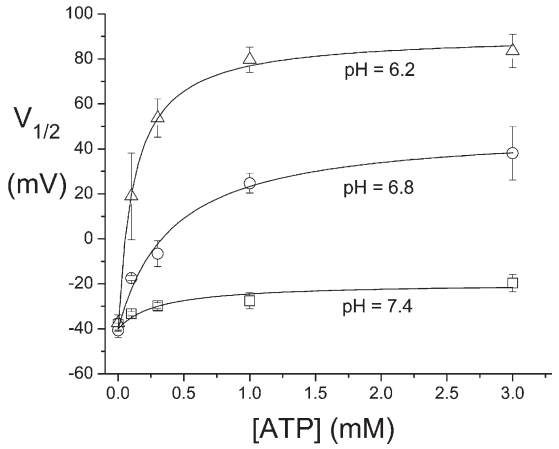

Figure 3. Dependence of the $V_{1/2}$ of the common-gate P_o^c–V curve on the ATP concentration in three different pH conditions. Each data point is the average from 3–7 patches. Solid curves are drawn according to a Michaelis-Menten equation with the ATP half-effective concentration and the saturated $V_{1/2}$ value of 0.31 mM and −20 mV (pH 7.4), 0.40 mM and +49 mV (pH 6.8), and 0.12 mM and +91 mV (pH 6.2).

open probability (namely $P_o^f \times P_o^c$) is plotted as a function of the preceding test voltage (Fig. 1 B). It is apparent that ATP shifts the overall voltage-dependent, open probability curve to more depolarized potential so that the channel is more difficult to open at the same voltage in the presence of ATP. The effect of ATP is small at the neutral pH, but the inhibition becomes large when the cytoplasmic pH is reduced.

To further study ATP regulations on the gating functions of CLC-1 we examine the common-gate P_o (P_o^c), which can be directly measured from the initial tail current of the recording traces obtained by using voltage protocol B (Fig. 2 A). Fig. 2 B shows the voltage dependence of P_o^c (P_o^c–V curve). ATP has only a small effect on the P_o^c–V curve of CLC-1 at a neutral pH. At pH 7.4, 1 mM ATP shifts the $V_{1/2}$ of the P_o^c–V curve by only 10 mV, from −38.0 ± 2.6 to −27.6 ± 3.6 mV. However, the ATP effect becomes larger when the intracellular pH is reduced. At pH 6.2, $V_{1/2}$ changes from a control value of −37.4 ± 3.6 mV (0 ATP) to +79.6 ± 5.6 mV (1 mM ATP). On the other hand, ATP has nearly no effect on the fast-gate P_o (P_o^f) in all three pH conditions (Fig. 2 B, insets).

To examine the concentration dependence of the ATP regulation on the common gate of CLC-1 at various pH conditions, we plot the $V_{1/2}$ of the P_o^c–V curves against ATP concentrations (Fig. 3). The ATP half-effective concentrations are 0.31, 0.40, and 0.12 mM in pH 7.4, 6.8, and 6.2, respectively. In the presence of physiological concentration of ATP, the shift of the P_o^c–V curve induced by lowering intracellular pH is robust. For example, in the presence of 1 mM ATP, there is an over 100-mV change in the $V_{1/2}$ from pH 7.4 (−27.6 ± 3.6 mV) to pH 6.2 (+79.6 ± 5.6 mV).

Thus, the ATP inhibition on the common gate of CLC-1 is enhanced by low pH. This effect is reversible, as can be seen from monitoring the ATP wash-in and wash-out processes at pH 6.8 (Fig. 4). Examining the kinetics reveals that the ATP wash-in process (as well as wash-out; unpublished data) cannot be well fitted to a single-exponential function (Fig. 4, red curve), indicating that there may be multiple steps in this combined ATP-pH regulation on the common gate of CLC-1. We have also attempted to compare the time courses of ATP inhibition (at pH 6.2) at voltages where P_o^c values are different (−40 vs. +40 mV). When fitting the first 5-s trace upon ATP application to a single-exponential function, the time constant at +40 mV was ~30% larger

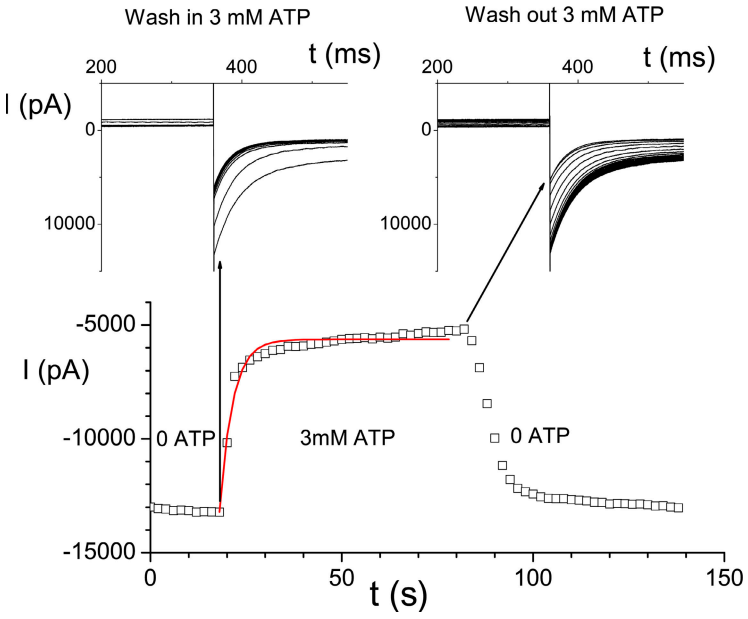

Figure 4. Reversible ATP inhibition on the CLC-1 common-gate activity at pH 6.8. Top panels show recording traces by a pulse protocol of +40 mV test voltage (300 ms), followed by the short pulse to +170 mV (400 μs), and finally the tail voltage step at −120 mV. The recorded traces were shown around the initial tail current for those traces during ATP wash-in (left) and wash-out (right). Each recording trace is separated by 2 s, and the initial value of the tail current in each trace is plotted against time at the bottom panel. The red curve represents a single-exponential fit with a time constant of 3.4 s, which does not fit the ATP wash-in process well. Three other patches show the same results from such ATP wash-in and wash-out experiments.

than that at −40 mV ($n = 4$). Because the inhibition process follows a two-exponential course, it requires more extensive study to determine if such a difference truly reflects a voltage-dependent change of ATP modulations.

DISCUSSION

We have used the *Xenopus* oocyte expression system to determine whether the recombinant CLC-1 channel can be modulated by intracellular pH and ATP. We employed excised inside-out patch recordings to gain an easy access to the cytoplasmic side of the channel. The results clearly show an inhibition of CLC-1 by a combined action of ATP and low pH; the ATP regulation effect is only small at neutral pH but becomes quite large when intracellular pH is reduced. This combined ATP-pH regulation appears to be mostly through the inhibition of the common gate, and a physiological concentration of ATP (for example, 1 mM) is nearly a saturated concentration in this regulation (Fig. 3). Thus, the effect may be viewed from another angle; namely, CLC-1 is inhibited by a low intracellular pH in the presence of ATP.

In the absence of ATP, a lower intracellular pH indeed renders the overall P_o of CLC-1 larger mostly due to an increase of P_o^f, an effect qualitatively similar to the intracellular H^+ effect on the fast gate of CLC-0 (Hanke and Miller, 1983), another voltage-sensitive CLC Cl^- channel. However, in the presence of ATP, the overall open probability of the CLC-1 channel is reduced by low intracellular pH due to the inhibition of P_o^c. This finding is consistent with the inhibition of the Cl^- conductance by a low intracellular pH in the native muscle membranes (Pedersen et al., 2004, 2005).

The effect of ATP regulation on CLC-1 has been reported previously using whole-cell recordings on the recombinant CLC-1 channels (Bennetts et al., 2005). In this early study, the shift of the P_o^c–V curve by saturated ATP at neutral pH (pH 7.2) was 50–60 mV. In Fig. 3, our excised patch experiments show only a 20-mV change of $V_{1/2}$ at the neutral pH (pH 7.4). One might have considered that these two studies provide discordant results regarding the extent of the shift by ATP. Because the shift of the P_o^c–V curve is ∼20, 85, and 130 mV at pH 7.4, 6.8, and 6.2, respectively (>10 mV shift per 0.1 pH unit), we expect a 40–50-mV shift of the P_o^c–V curve at pH 7.2 for our experiments. Given the very different techniques used (whole-cell vs. excised, inside-out patch recordings), we consider the discrepancy (50–60 mV vs. 40–50 mV) between these two studies to be within experimental error range.

The regulation of the CLC-1 common gating by cytoplasmic ATP was thought to result from the ATP binding to the cystathionine β-synthase (CBS) domains at the C terminus of CLC-1. The CBS domain is conserved throughout CLC family members (Bennetts et al., 2005), and the crystal structures of the C-terminal cytoplasmic portion of CLC-0 and CLC-5 have recently been solved in CLC-0 and CLC-5 (Meyer and Dutzler, 2006; Meyer et al., 2007). Though the structural study demonstrated the binding of nucleotides to the C-terminal region of CLC-5 (Meyer et al., 2007), no functional effect of ATP regulation of CLC-5 has been reported. So far, the inhibition of CLC-1 by ATP remains the best example of ATP regulations of the CLC family members. The results presented in this study have demonstrated for the first time a clear, reversible action of ATP on CLC-1 through continuously monitoring the ATP wash-in and wash-out processes (Fig. 4).

The wash-in and wash-out processes of ATP regulation of the CLC-1 common gate, however, cannot be well fitted to a single-exponential function (Fig. 4), raising the possibility that the combined ATP-pH action may require multiple kinetic steps. This is reasonable if the effect requires both ATP binding to its binding site and protonation of certain titratable groups in the channel protein. If these two processes are independent (for example, the titratable group is outside the ATP-binding pocket), one might expect that the apparent ATP half-effective concentrations do not show a strong dependence on the pH, as indeed revealed in Fig. 3. However, it will require more detailed studies to explore the mechanism underlying the inhibition of the CLC-1 common gate by the combined action of cytoplasmic ATP and pH.

We thank Drs. Xiao-Dong Zhang and Wei-Ping Yu for technical assistances.

This work was supported by a grant from National Institutes of Health (GM65447).

Olaf S. Andersen served as editor.

Submitted: 2 May 2007
Accepted: 9 July 2007

REFERENCES

Accardi, A., and M. Pusch. 2000. Fast and slow gating relaxations in the muscle chloride channel CLC-1. *J. Gen. Physiol.* 116:433–444.

Bennetts, B., G.Y. Rychkov, H.L. Ng, C.J. Morton, D. Stapleton, M.W. Parker, and B.A. Cromer. 2005. Cytoplasmic ATP-sensing domains regulate gating of skeletal muscle ClC-1 chloride channels. *J. Biol. Chem.* 280:32452–32458.

Chen, T.Y. 1998. Extracellular zinc ion inhibits ClC-0 chloride channels by facilitating slow gating. *J. Gen. Physiol.* 112:715–726.

Duffield, M., G. Rychkov, A. Bretag, and M. Roberts. 2003. Involvement of helices at the dimer interface in ClC-1 common gating. *J. Gen. Physiol.* 121:149–161.

Hanke, W., and C. Miller. 1983. Single chloride channels from *Torpedo electroplax*. Activation by protons. *J. Gen. Physiol.* 82:25–45.

Hutter, O.F., and A.E. Warner. 1967a. The effect of pH on the 36-Cl efflux from frog skeletal muscle. *J. Physiol.* 189:427–443.

Hutter, O.F., and A.E. Warner. 1967b. The pH sensitivity of the chloride conductance of frog skeletal muscle. *J. Physiol.* 189:403–425.

Koch, M.C., K. Steinmeyer, C. Lorenz, K. Ricker, F. Wolf, M. Otto, B. Zoll, F. Lehmann-Horn, K.H. Grzeschik, and T.J. Jentsch. 1992. The skeletal muscle chloride channel in dominant and recessive human myotonia. *Science.* 257:797–800.

Li, Y., W.P. Yu, C.W. Lin, and T.Y. Chen. 2005. Oxidation and reduction control of the inactivation gating of *Torpedo* ClC-0 chloride channels. *Biophys. J.* 88:3936–3945.

Meyer, S., and R. Dutzler. 2006. Crystal structure of the cytoplasmic domain of the chloride channel ClC-0. *Structure.* 14:299–307.

Meyer, S., S. Savaresi, I.C. Forster, and R. Dutzler. 2007. Nucleotide recognition by the cytoplasmic domain of the human chloride transporter ClC-5. *Nat. Struct. Mol. Biol.* 14:60–67.

Palade, P.T., and R.L. Barchi. 1977. Characteristics of the chloride conductance in muscle fibers of the rat diaphragm. *J. Gen. Physiol.* 69:325–342.

Pedersen, T.H., O.B. Nielsen, G.D. Lamb, and D.G. Stephenson. 2004. Intracellular acidosis enhances the excitability of working muscle. *Science.* 305:1144–1147.

Pedersen, T.H., F. de Paoli, and O.B. Nielsen. 2005. Increased excitability of acidified skeletal muscle: role of chloride conductance. *J. Gen. Physiol.* 125:237–246.

Rychkov, G.Y., M. Pusch, D.S. Astill, M.L. Roberts, T.J. Jentsch, and A.H. Bretag. 1996. Concentration and pH dependence of skeletal muscle chloride channel ClC-1. *J. Physiol.* 497:423–435.

Sejersted, O.M., and G. Sjogaard. 2000. Dynamics and consequences of potassium shifts in skeletal muscle and heart during exercise. *Physiol. Rev.* 80:1411–1481.

Steinmeyer, K., C. Ortland, and T.J. Jentsch. 1991. Primary structure and functional expression of a developmentally regulated skeletal muscle chloride channel. *Nature.* 354:301–304.

Zhang, X.D., Y. Li, W.P. Yu, and T.Y. Chen. 2006. Roles of K149, G352, and H401 in the channel functions of ClC-0: testing the predictions from theoretical calculations. *J. Gen. Physiol.* 127:435–447.